Monatshefte für Chemie - Chemical Monthly
https://doi.org/10.1007/s00706-021-02778-8

ORIGINAL PAPER

Synthesis of novel methoxyether derivative of isopulegol in a packed-bed flow reactor

Upenyu Guyo[1] · **Buyiswa G. Hlangothi**[1] · **Ben Zeelie**[1]

Received: 15 September 2020 / Accepted: 26 April 2021

Abstract

8–Methoxymenthan–3–ol was synthesised in a packed-bed flow reactor by the reaction of isopulegol and methanol in the presence of amberlyst-15 dry hydrogen form catalyst. Key parameters that affect isopulegol conversion and 8–methoxymenthan–3–ol formation were investigated and optimised. The reaction was found to be highly temperature-dependent, and to be less dependent of isopulegol: methanol molar ratio. Higher temperatures coupled with rapid flow rates resulted in higher isopulegol conversion. The optimum working temperature in the reactor was 57 °C and a maximum yield of 51.8% of 8–methoxymenthan–3–ol was obtained in 27.4 min at a flow rate of 3.6 cm^3/min.

Graphic abstract

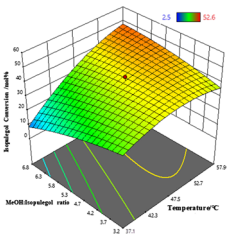

Keywords Isopulegol · Methanol · Amberlyst-15 dry hydrogen · Packed bed flow reactor · 8–Methoxymenthan–3–ol

Introduction

Although South Africa is rich in natural resources and has a significant petrochemical industry, most fine chemicals are imported from overseas as there are very few fine chemical industries. There is therefore a pronounced interest to use these abundant natural resources in the development and evaluation of a range of value-added compounds for use in sensitive applications. The use of these natural resources ensures economic self-sustenance as this develops a sustainable business concept from the cultivation of plant material through the isolation of rich oil from the plant material, to the conversion of the oil (or components thereof) into the industry and consumer products. While there is a significant motivation for such research from a job creation point of view, especially in a developing region such as Southern Africa, there is also significant scientific motivation for undertaking a project of this nature. Thus the use of natural feedstocks can lead to the development of environmentally benign and sustainable materials.

One important natural feedstock which is widely used in the synthesis of high-value chemicals is citronellal, a monoterpenoid aldehyde. Citronellal (**1**), also known as rhodinal (3,7–dimethyloct–6–enal), is obtained from *Corymbia Citriodora Hill* oil, *Johnson Cymbopogon Nardus* oil, and *Java Citronella* oil by steam distillation to give a non-racemic mixture of *R* and *S* enantiomers [1]. Citronellal is a repellent against mosquitoes and has been widely used as an insect repellent [2]. It also works effectively as an antifungal and has been used frequently in pharmaceuticals [3]. Furthermore, it is a very versatile compound in

✉ Upenyu Guyo
upguyo@gmail.com

[1] Nelson Mandela University, PO Box 77000, Port Elizabeth 6031, South Africa

Published online: 19 May 2021

perfumery and cosmetic applications as well as a precursor in the synthesis of several important terpenes. Moreover, citronellal can be transformed chemically or biochemically into important compounds such as citronellol [4–7], isopulegol [8–14], menthol [15–19], and *p*–menthane–3,8–diol (**6**) [20–22] which have numerous applications industrially such as children's products, pharmaceutics, insect repellents, food products, cosmetics, personal care products [2, 7]. Besides being a versatile starting material for the synthesis of numerous compounds, citronellal is cheap and readily available. Together with its derivatives, it becomes a possible suitable starting material for the production of the essential fine chemicals.

Isopulegol (**2**) is a monoterpenic alcohol derived from citronellal through a cyclisation reaction [9–14]. Cyclisation of (+)–citronellal yields four diastereoisomers namely (−)–isopulegol, (+)–neo–isopulegol, (+)–iso–isopulegol, and (+)–neoiso–isopulegol, whereas, cyclisation of (−)–citronellal yields (+)–isopulegol, (−)–neo–isopulegol, (−)–iso–isopulegol, and (−)–neoiso–isopulegol as shown in Scheme 1. Of the four isomers, isopulegol and neo–isopulegol are the main isomers.

Isopulegol is an important material employed in the manufacture of fragrances in the flavour and perfume industry. It is a useful starting material for the synthesis of three isomers of 5,9–dimethylpentadecane, which are the main sex pheromone components [23]. It is also an important intermediate in the synthesis of the (−)–menthol isomer which is employed in toothpaste, cigarettes, sweets, agrochemicals, pharmaceutical, and personal care products.

As part of our overall research goals, we report herein the synthesis of a novel ether derivative of isopulegol using continuous flow technology. Here, we take advantage of continuous flow technology which offers chemistry safety, processing time reduction, easy scale-up, reproducibility, and process overall yield improvement [24–28]. The synthesis method involves the etherification of isopulegol with methanol in flow using amberlyst-15 catalyst (Scheme 2). The ether derivatives are in the meantime being investigated in our research group for a variety of applications including further derivatisation.

Scheme 2

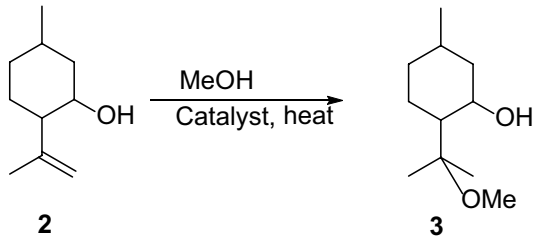

2 **3**

Scheme 1

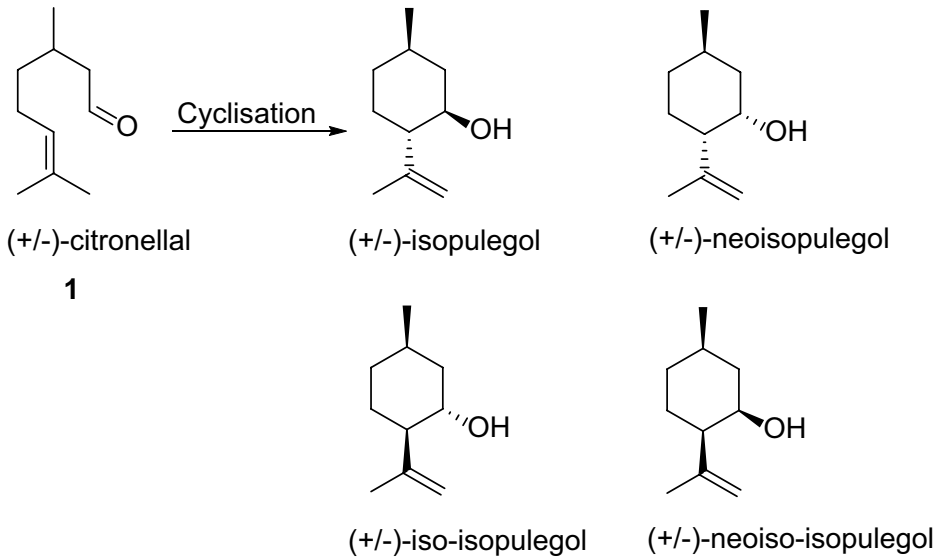

(+/-)-citronellal (+/-)-isopulegol (+/-)-neoisopulegol

1

(+/-)-iso-isopulegol (+/-)-neoiso-isopulegol

2

Results and discussion

Synthesis of 8–methoxymenthan–3–ol in a packed-bed reactor

The etherification of isopulegol with methanol in a packed-bed reactor was investigated in the experimental domain given in Table 1.

The investigation was carried out over a total of 24 experiments (Table 2). Several replicate experiments were included in the 24 experiments to check the long-term performance of the amberlyst-15 catalyst. The experimental settings used for this investigation together with the actual experimental results are shown in Table 2.

Unlike the batch reactor, it is not possible to separate the effects of mixing and residence time in the packed-bed reactor. The degree of mixing in the packed-bed reactor is determined by the linear flow velocity of reagents through the bed: as the flow rate increases so does the degree of mixing. At the same time, however, the residence time in the reactor is reduced. Figure 1 illustrates the effect of increasing flow rate at constant temperature and MeOH: isopulegol molar ratio.

The results depicted in Fig. 1 clearly show that both isopulegol conversion and 8–methoxy–menthan–3–ol formation decreases continuously with increasing flow rate. The effect of increasing temperature, whilst keeping the flow rate and the MeOH: isopulegol molar ratio constant (Fig. 2) shows that isopulegol conversion increases with increasing reaction temperature as expected, but the amount of 8–methoxymenthan–3–ol appears to reach a maximum at approximately 56 °C before starting a declining trend.

The effect of increasing the amount of methanol relative to isopulegol (Fig. 3) on both the isopulegol conversion and the amount of 8–methoxymenthan–3–ol

Table 1 Experimental domain

	Temperature/°C	Flow rate/cm^3 min^{-1}	MeOH: isopulegol molar ratio
Min point	30	2	2
Max point	65	10	8

Table 2 Experimental settings and results—packed-bed reactor

Entry	Temperature/°C	Flow rate/cm^3 min^{-1}	Residence time/min	MeOH: isopulegol molar ratio	Isopulegol conversion /%	Ether yield /%	Ether selectivity/%
1	60	9	10.95	3	57.9	42.6	69.1
2	48	2	49.27	5	59.4	52.6	83.6
3	30	6	16.42	5	5	2.5	47
4	48	6	16.42	2	41	38.1	87.3
5	65	6	16.42	5	59.3	38.6	61.2
6	60	3	32.85	7	61.6	43.4	66.3
7	48	6	16.42	5	42.5	38.1	84.4
8	48	6	16.42	8	30.2	28.1	87.5
9	30	6	16.42	5	5.6	4.8	80.3
10	35	3	32.85	7	10.8	8.7	76
11	48	6	16.42	5	46.3	43.1	87.6
12	35	3	32.85	3	14.7	12.8	82
13	48	6	16.42	2	42.5	38.1	84.4
14	48	6	16.42	8	35.5	32.6	86.2
15	48	6	16.42	5	37.8	35	87.3
16	48	10	9.85	5	20.7	19.1	86.5
17	60	9	10.95	7	58.4	49.1	79.1
18	60	3	32.85	3	63.2	38.8	57.7
19	48	2	49.27	5	60.6	48.1	74.8
20	35	9	10.95	3	2.6	2.7	96.3
21	65	6	16.42	5	56.3	43.5	72.6
22	48	10	9.85	5	25.9	25	90.7
23	48	6	16.42	5	46.3	43	87.4
24	35	9	10.95	7	2.9	2.2	71.5

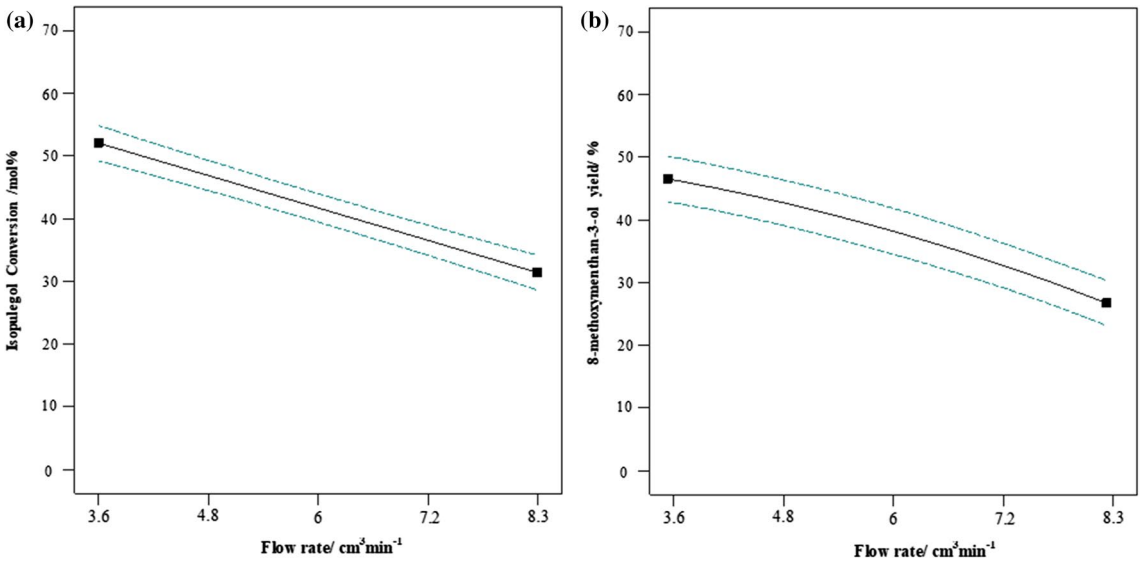

Fig. 1 Effect of flow rate on isopulegol conversion **a** and 8–methoxymenthan–3–ol formation **b**; temperature = 47.5 °C; MeOH: isopulegol molar ratio = 5

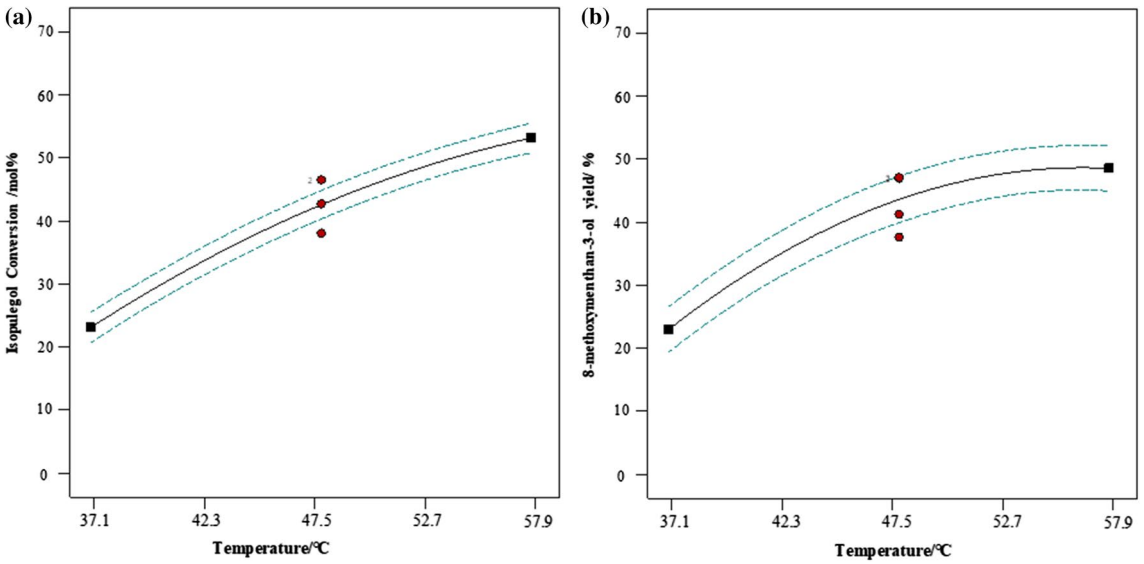

Fig. 2 Effect of increasing temperature on isopulegol conversion **a** and 8–methoxymenthan–3–ol yield **b**; flow rate = 6 cm^3/min; MeOH: isopulegol molar ratio = 5

formation shows that there appears to be an optimum MeOH: isopulegol ratio at around four equivalents MeOH to one equivalent isopulegol.

The observed decrease in isopulegol conversion and 8–methoxymenthan–3–ol formation is probably a simple dilution effect as the two curves in Fig. 3 seem to mirror each other.

Response surface modelling

The obtained experimental data (Table 2) were fitted to the general second-order polynomial model (Eq. (1)) following a step-wise regression analysis using the Design Expert V 11.0 software package:

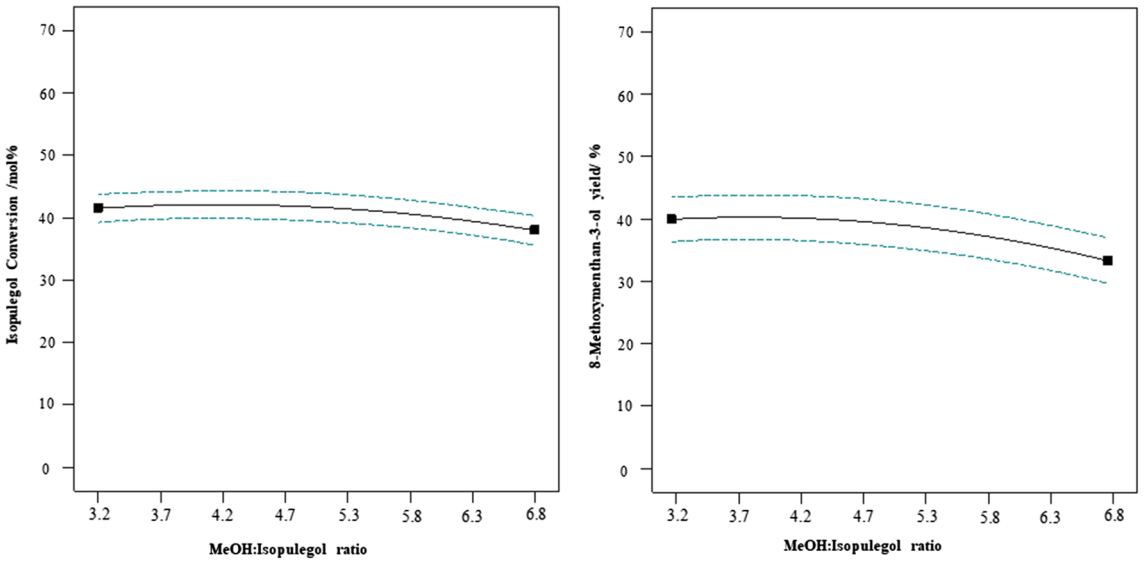

Fig. 3 Effect of increasing MeOH: isopulegol ratio on isopulegol conversion and 8–methoxymenthan–3–ol formation; temperature = 47.5 °C; flow rate = 6 cm^3/min

$$Y = \beta_0 + \beta_1 X_1 + \beta_2 X_2 + \beta_3 X_3 + \beta_4 X_1 X_2 + \beta_5 X_1 X_3 + \beta_6 X_2 X_3 + \beta_7 X_1^2 + \beta_8 X_2^2 + \beta_9 X_3^2, \quad (1)$$

where β_i = model coefficients; X_1 = temperature; X_2 = flow rate; X_3 = MeOH: isopulegol mol ratio.

The results of the Analysis of Variance are summarised in Table 3 for the conversion of isopulegol results, and in Table 4 for 8–methoxymenthan–3–ol formation results.

All of the insignificant terms (p value > 0.05) were disregarded to give the final regression models (Eqs. (2) and (3)) in terms of coded factors:

$$\%\text{isopulegolconversion} = 41.70 + 15.05X_1 - 10.34X_2 - 1.78X_3 - 6.36X_1X_3 - 5.70X_2X_3 - 3.76X_1^2 - 1.96X_3^2, \quad (2)$$

$$\%8-\text{methoxymenthan}-3-\text{ol} = 39.67 + 10.97X_1 - 8.49X_2 - 2.86X_3 + 4.91X_1X_2 + 8.63X_1X_3 + 4.33X_2X_3 - 6.25X_1^2 - 1.55X_2^2 - 2.22X_3^2. \quad (3)$$

Table 3 ANOVA data for isopulegol conversion

Source	Sum of squares	d*f*	Mean square	*F* value	*p* value	
Model	9072.32	7	1296.05	145.32	< 0.0001	Significant
X_1-Temperature	3401.02	1	3401.02	381.34	< 0.0001	
X_2-Flow rate	1661.51	1	1661.51	186.30	< 0.0001	
X_3-MeOH: isopulegol ratio	58.44	1	58.44	6.55	0.0227	
$X_1 X_3$	288.52	1	288.52	32.35	< 0.0001	
$X_2 X_3$	255.34	1	255.34	28.63	0.0001	
X_1^2	349.42	1	349.42	39.18	< 0.0001	
X_3^2	91.47	1	91.47	10.26	0.0064	
Lack of fit	41.90	5	8.38	0.9092	0.5157	Not significant
R^2	0.9864					
Adjusted R^2	0.9796					
Predicted R^2	0.9692					
Adequate precision	36.7838					

Table 4 ANOVA data for 8–methoxymenthan–3–ol formation

Source	Sum of squares	df	Mean square	F value	p value	
Model	4830.79	9	536.75	56.53	< 0.0001	Significant
X_1-temperature	1613.71	1	1613.71	169.96	< 0.0001	
X_2-flow rate	942.33	1	942.33	99.25	< 0.0001	
X_3-MeOH: isopulegol ratio	102.13	1	102.13	10.76	0.0073	
$X_1 X_2$	180.46	1	180.46	19.01	0.0011	
$X_1 X_3$	422.04	1	422.04	44.45	< 0.0001	
$X_2 X_3$	125.42	1	125.42	13.21	0.0039	
X_1^2	855.31	1	855.31	90.08	< 0.0001	
X_2^2	54.85	1	54.85	5.78	0.0350	
X_3^2	103.16	1	103.16	10.87	0.0071	
Lack of fit	5.08	2	2.54	0.2300	0.7991	Not significant
R^2	0.9788					
Adjusted R^2	0.9615					
Predicted R^2	0.9297					
Adequate precision	22.1484					

p Values of less than 0.05 ($p = 0.0001$) showed that the models were statistically significant. This was further supported by higher regression coefficients of 0.9864 (isopulegol conversion) and 0.979 (8–methoxymenthan–3–ol formation). Small variations of 0.0104 (isopulegol conversion) and 0.0318 (8–methoxymenthan–3–ol formation) between predicted R^2 and adjusted R^2 are further evidence for the significances of the models. In addition, the high lack of fit F values of 0.5157 (isopulegol conversion) and 0.7991 (8–methoxymenthan–3–ol formation) implied higher probabilities of the models fitting the data. Furthermore, an adequate precision greater than 4 is desirable as it measures the signal-to-noise ratio. Based on the above results, adequate precision values of 36.7838 (isopulegol conversion) and 22.1484 (8–methoxymenthan–3–ol formation) were obtained showing adequate signals.

Model validation

The normal probability plots for the residuals (observed values − values predicted by the model) are shown in Fig. 4 for isopulegol conversion and in Fig. 5 for 8–methoxymenthan–3–ol formation. Both these plots show that the residuals fall on, or nearly on a straight line, implying that the residuals are normally distributed, hence that the observed data are normally distributed.

In addition to the normal probability plots, a plot of the predicted versus actual values shows a close agreement between the two for the two models (Fig. S10 and S11). Also, plots of predicted responses versus the residuals (Fig. S12 and S13) do not show any particular trend (random distribution). These graphical tests show that the two models do not show any abnormal behaviour and can therefore be used for analysing the data.

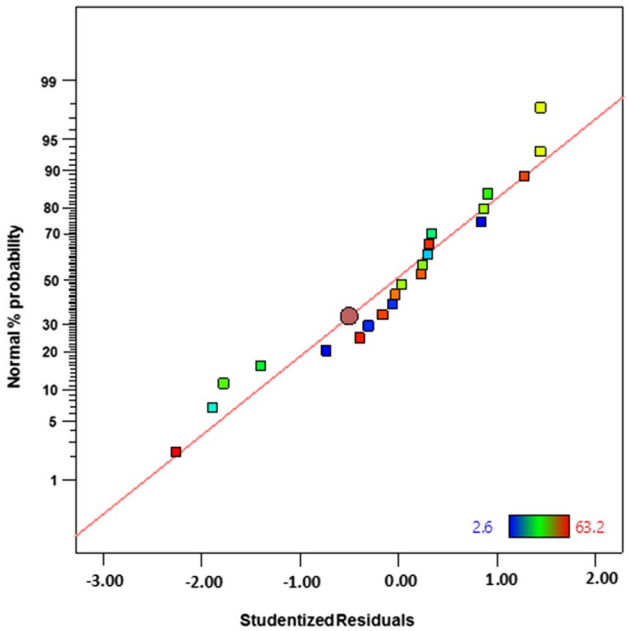

Fig. 4 Normal probability plot of residuals—isopulegol conversion model

Perturbation and three-dimensional response surface plots

Figure 6 shows the perturbation plots obtained using the Design Expert software. The perturbation plot shows that the temperature (X_1) and flow rate (X_2) had significant influences on both isopulegol conversion and 8–methoxymenthan–3–ol formation whilst MeOH to isopulegol molar ratio (X_3) had a slight influence on both.

Figures 7 and 8 show the 3-dimensional plots for isopulegol conversion and 8–methoxymenthan–3–ol formation

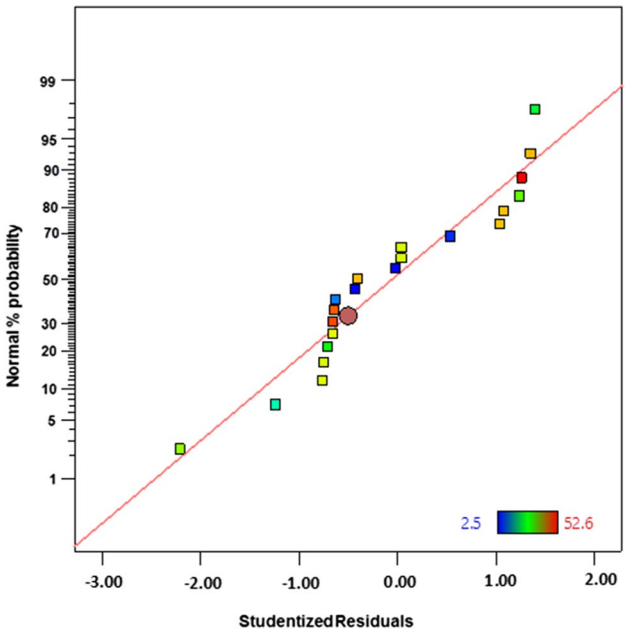

Fig. 5 Normal probability plot of residuals—8–methoxymenthan–3–ol formation model

as a function of temperature and methanol: isopulegol molar ratio.

The 3D response surface plots are in full agreement with earlier observations, namely an increase in isopulegol conversion with increasing reaction temperature, with the MeOH: isopulegol ratio having virtually little effect on the conversion. For 8–methoxymenthan–3–ol formation, the general trend mirrors that observed for isopulegol conversion, except that there is a clear maximum at 57 °C. This observation can probably be explained in terms of the larger propensity for dehydration of 8–methoxymenthan–3–ol (**3**) to form the alkene **4** (Scheme 3) as the reaction temperature increases above 57 °C.

Optimisation of the reaction parameters

The desirability function on the Design Expert software was used to examine the optimum reaction conditions for the synthesis of 8–methoxymenthan–3–ol in a packed-bed flow reactor. The optimum conditions were deduced to be a temperature of 57.9 °C, a flow rate of 3.6 cm^3/min and MeOH–isopulegol molar ratio of 3.9 for isopulegol conversion of 64.0% and a temperature of 45.3 °C, a flow rate of 3.6 cm^3/min and MeOH–isopulegol molar ratio of 3.2 for an 8–methoxymenthan–3–ol yield of 51.8%.

Characterisation of 8–methoxymenthan–3–ol

The etherification of isopulegol involves the electrophilic addition of methanol across the double bond. The identity of the 8–methoxymenthan–3–ol product is evidenced by the disappearance of alkene peaks on the IR spectrum of 8–methoxymenthan–3–ol (Fig. S4). The infrared spectrum shows an O–H stretching band at 3454 cm^{-1} and a C–O–C stretching band characteristic of a methoxy group at 1051 cm^{-1}. The peak at around 1455–1367 cm^{-1} is characteristic of a C–H bend showing the presence of methylene and methyl groups and the one at 1161 cm^{-1} shows C–OH stretching.

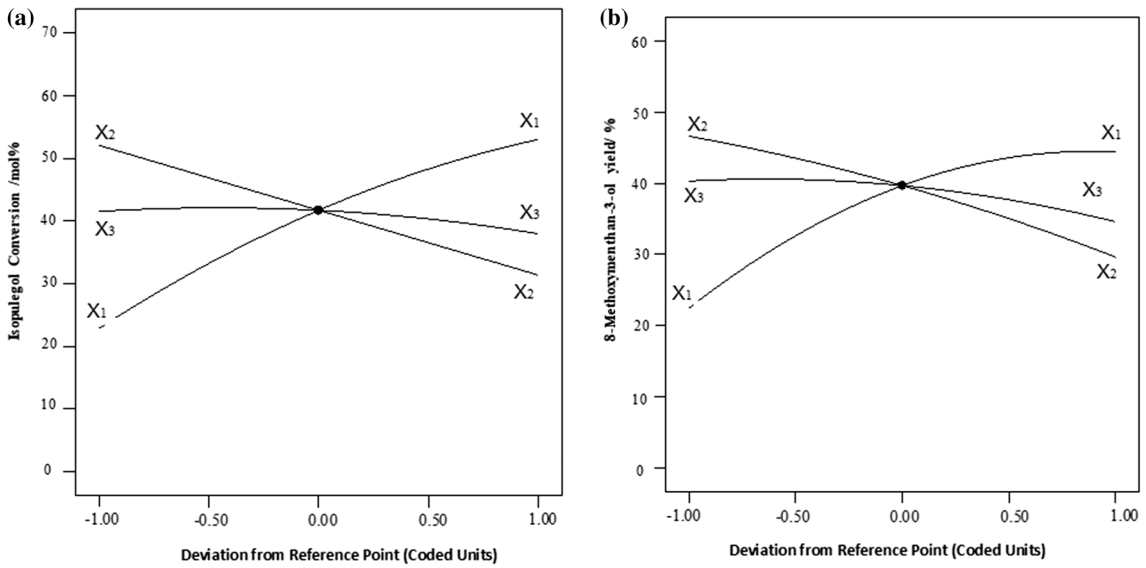

Fig. 6 Perturbation plots of the employed models, isopulegol conversion **a**, and 8–methoxymenthan–3–ol formation **b**

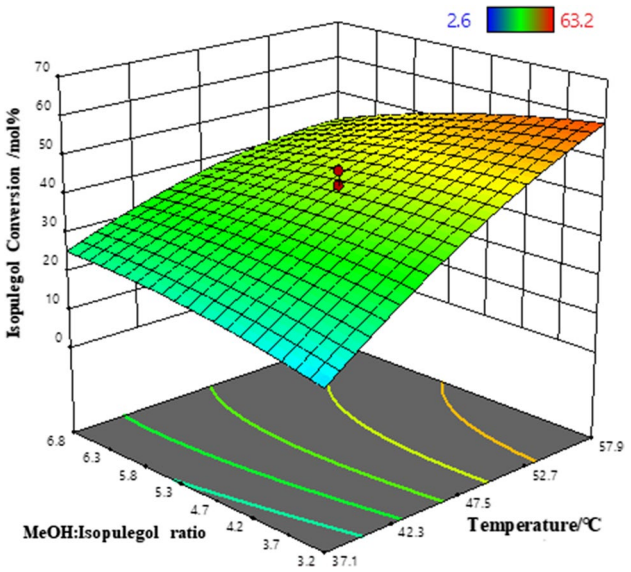

Fig. 7 3-D response surface plot for isopulegol conversion

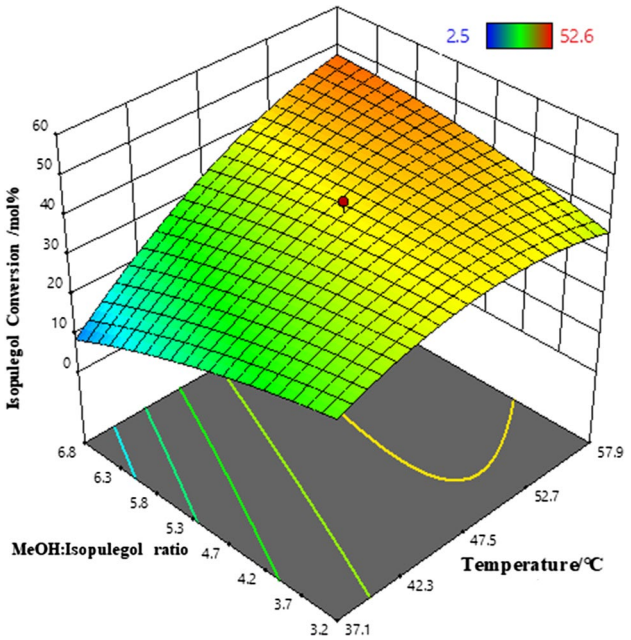

Fig. 8 3-D response surface plot for 8–methoxymenthan–3–ol formation

8–Methoxymenthan–3–ol's mass spectrum showed a weak molecular ion peak at $m/z = 187.1$ corresponding to $C_{11}H_{22}O_2^+$ and a base peak at $m/z = 73.1$ corresponding to $C_4H_9O^+$ (Fig. S5). The peak at $m/z = 171$ corresponds to $C_{10}H_{19}O_2$ which is due to the loss of the methyl group from the molecular ion.

The ^{1}H NMR spectrum revealed the presence of the new expected signals, three methyl protons of

Scheme 3

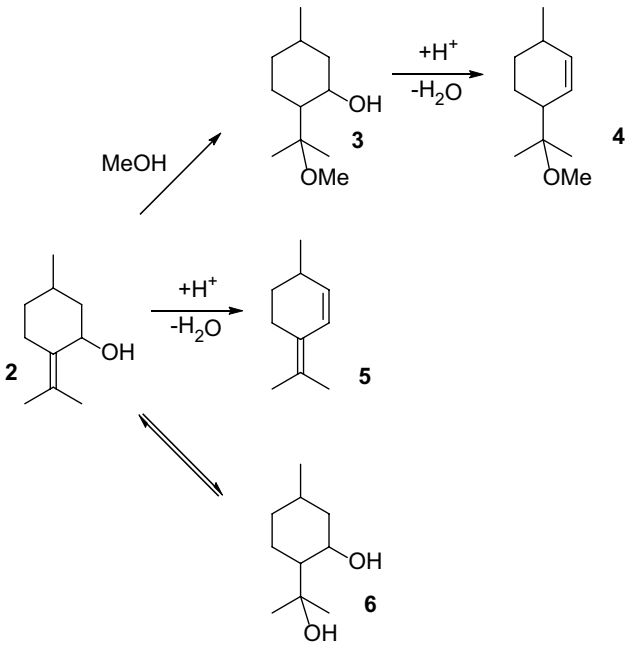

8–methoxymenthan–3–ol as a singlet resonance at $\delta_H = 3.18$ ppm, and the methyl protons of the isopropyl group were seen at 1.11 and 1.14 ppm as singlets (Fig. S6). The H–3 proton resonated as a doublet of a triplet at 3.57 ppm ($J = 10.2$ and 4.2 Hz) due to splitting by the neighbouring protons. This proton is attached to the carbon atom which is bonded to an OH group and hence its signal appears downfield at 3.57 ppm. The ^{13}C NMR spectrum confirms the identity and purity of the isolated product by the non-appearance of alkene peaks between $\delta_C = 101.2$ and 146 ppm (Fig. S7). The methoxy group resonated at 48.5 ppm as confirmed by an HSQC NMR spectrum (Fig. S8).

Conclusion

Synthesis in the packed-bed flow reactor was found to depend highly on temperature and significantly on the flow rate (residence time). Isopulegol conversion and 8–methoxymenthan–3–ol formation decrease with an increasing flow rate. Higher temperatures at longer residence times resulted in higher isopulegol conversions. Several side reactions, however, became significant which reduced ether selectivity. These side reactions include dehydration of isopulegol to 3–methyl–6–(prop–1–en–2–yl)cyclohexene (**5**) and dehydration of 8–methoxymenthan–3–ol to 3–(2–methoxypropan–2–yl)–6–methylcyclohexene (**4**). Other side reactions though not very significant include

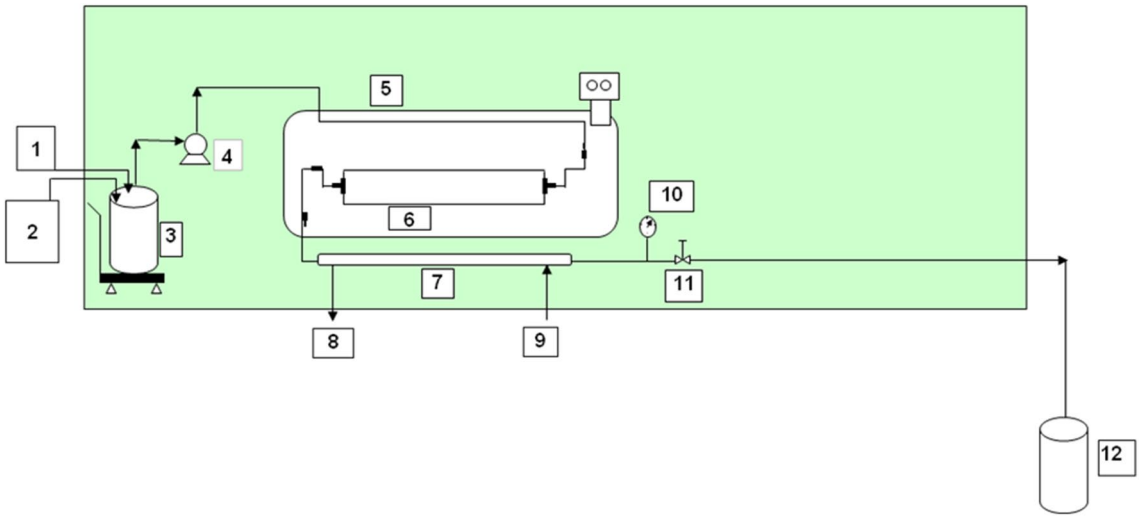

Fig. 9 Fixed-bed reactor for 8–methoxymenthan–3–ol synthesis. 1 = Methanol feed; 2 = Isopulegol/toluene feed; 3 = Isopulegol/toluene/methanol premix; 4 = HPLC pump; 5 = Oil bath; 6 = Reactor packed with amberlyst-15 catalyst; 7 = Heat exchanger, 8 = Chilled water out; 9 = Chilled water in; 10 = Pressure gauge (5 bar); 11 = Heat exchanger; 12 = Reactor product

the formation of *p*–menthane–3,8–diol (**6**) from isopulegol. The maximum working temperature in the reactor before the decline of 8–methoxymenthan–3–ol formation was 57 °C and the maximum of 51.8% was obtained at a flow rate of 3.6 cm^3/min.

Experimental

Amberlyst-15 dry hydrogen form (Sigma-Aldrich, concentration of acid sites ≥ 4.7 eq/kg, nitrogen BET: surface area 53 m^2/g; average pore diameter 300 Å; total pore volume 0.40 cc/g), isopulegol (University of Cape Town, 94.1%), methanol (Merck, 95–98%), toluene (Merck, 99.8%), *n*–hexane (Merck, Analytical Reagent grade), ethyl acetate (Sigma-Aldrich, Analytical Reagent grade), sulfuric acid (Merck). All solvents were distilled from their respective suitable drying agents and stored under molecular sieves.

Gas chromatographic analyses were performed on an Agilent Gas chromatograph, equipped with a flame ionisation detector. Data were acquired from the detector using a Mecer personal computer equipped with Agilent Chemstation software for the recording and integration of chromatograms. IR spectra were recorded on a Bruker Platinum Tensor 27 spectrophotometer with an ATR fitting. Typically 100 scans were collected for each sample. The characteristic peaks were recorded in wavenumbers. NMR spectra were obtained with a Bruker Ultrashield Plus, long hold-time operating at 400 MHz. Unless mentioned otherwise, deuterated chloroform was used as a solvent. Tetramethylsilane (TMS) was used as the internal standard. Chemical shifts are reported in parts per million downfield from TMS and coupling constants (*J*) are given in Hz. NMR-signals multiplicities are abbreviated as follows: d = doublet; dd = doublet of doublets; dt = doublet of triplet; m = multiplet; q = quartet; s = singlet.

Fixed-bed flow reactor setup

The tubular packed-bed reactor was made from 1/4 and 1/8 inch stainless steel tubing (Fig. 9). The reactor consisted of two HPLC pumps; one used to pump the reaction feed and the other one to pump chilled water to cool the reactor effluent. The reactor consisted of three compartments: (1) A pre-heater compartment which was a coiled 1/8 inch stainless steel tubing to heat the feed to the required temperature before entering the reactor compartment. A thermocouple was connected at the end of the pre-heater compartment to allow for monitoring of the temperature of the feed. (2) A 98.54 cm^3 reactor volume compartment which was fabricated using a six-metre coiled 1/4 inch outside diameter and 0.035 inch wall thickness stainless steel tubing packed with the catalyst, amberlyst 15 dry hydrogen form (60.11 g). At its end was another thermocouple to measure the temperature of the reactor effluent. (3) A heat exchanger at the end of the catalyst bed was used for cooling the reactor product stream. A pressure sensor and an automatic valve were used to maintain the pressure of the system and were positioned after the heat exchanger.

Typical procedure

The oil bath was switched on and temperature set following the experiments specified by a central composite design (CCD). The chilled water bath and the high-performance liquid chromatography (HPLC) pump which pumped the chilled water to the heat exchanger were switched on. The pressure was set at 5 bar for all the experiments. Isopulegol (30.0 g, 199.66 mmol), methanol (as per CCD), and 70 cm^3 toluene were mixed thoroughly by shaking to obtain a homogenous mixture. The reactor system was first flushed with toluene and equilibrated to the required temperatures. Thermocouples were used to measure temperature. The reaction mixture was then pumped into the reactor system by an HPLC pump. The flow rates used were as per CCD. The reactor effluent was collected in a receiving container, and the system flushed with toluene to cater for residual reaction products remaining in the system. Toluene and unreacted methanol were removed on a rotorvapour and a sample analysed by gas chromatography (GC). In between the individual runs, the reactor system packed with amberlyst-15 catalyst was washed with 10% H_2SO_4: MeOH (100 cm^3) at a flow rate of 5 cm^3/min followed by flushing with 100 cm^3 toluene in preparation for the next run.

8–Methoxymenthan–3–ol (3, $C_{11}H_{22}O_2$) FT-IR: $\overline{\nu}$ = 3454, 2926–2868, 1054, 906, 731 cm^{-1}; ^{1}H NMR (400 MHz, $CDCl_3$): δ = 0.83 (3H, d, J = 4.0 Hz, C^7H_3), 0.87—0.93 (3H, m, C^6HH, C^5H, C^2HH), 1.11, 1.14 (6H, 2 × s, C^9H_3, $C^{10}H_3$), 1.16–1.26 (2H, m, C^1H, C^4H), 1.45–1.62 (2H, m, C^5HH, C^6HH), 1.89 (1H, br t, C^2HH), 3.18 (3H, s, $OC^{11}H_3$), 3.57 (1H, dt, J = 10.2, 4.2 Hz, C^3H) ppm; ^{13}C NMR (100 MHz, $CDCl_3$): δ = 19.8, 23.4 (C–9, C–10), 22.0 (CH_3), 26.6, 34.7 (C–5, C–6), 30.9 (C–1), 43.8 (C–2), 48.3 (OCH_3), 50.2 (C–4), 71.9 (C–3), 80.6 (C–8) ppm.

Supplementary Information The online version contains supplementary material available at https://doi.org/10.1007/s00706-021-02778-8.

Acknowledgements In loving memory of Professor Ben Zeelie†. The authors would like to thank InnoVenton, and Nelson Mandela University Research Office for financial support.

References

1. Lenardao EJ, Botteselle GV, De Azambuja F, Perin G, Jacob RG (2007) Tetrahedron 63:6671
2. Kim K-J, Kang C-S, Lee J-K, Kim Y-R, Han H-Y, Yun HK (2005) Entomol Res 35:117
3. Nakahara K, Alzoreky NS, Yoshihashi T, Nguyem HTT, Trakoontivakorn G (2003) Japan Agric Res Q 37:249
4. Corey E, Ensley HE, Suggs WJ (1976) J Org Chem 41:39
5. Kaur S, Rana S, Pal H, Rani D (2011) Z Naturforsch C J Biosci 66:260
6. Brito RG, Guimaraes AG, Quintans JSS, Santos MRV, De Sousa DP, Badaue-Passos D Jr, de Lucca JW, Brito FA, Barreto EO, Quintans LJ Jr (2012) J Nat Med 66:637
7. Katsukawa M, Nakata R, Koeji S, Hori K, Takahashi S, Inoue H (2011) Biosci Biotechnol Biochem 75:1010
8. Jacob RG, Perin G, Loi LN, Pinno CS, Lenardao EJ (2003) Tetrahedron Lett 44:3605
9. Yongzhong Z, Yuntong N, Jaenicke S, Chuah G (2005) J Catal 229:404
10. Mäki-arvela P, Kumar N, Nieminen V, Sjöholm R, Salmi T, Yu D (2004) J Catal 225:155
11. Coman SM, Patil P, Wuttke S, Kemnitz E (2009) Chem Commun 460
12. Fuentes M, Magraner J, Las Pozas CD, Roque-Malherbe R (1989) Appl Catal 47:367
13. Kozhevnikova EF, Kozhevnikov IV, Gusevskaya EV (2004) Catal Commun 5:425
14. Chuah GK, Liu SH, Jaenicke S, Harrison LJ (2001) J Catal 200:352
15. Cirujano F, Xamena LF, Corma A (2012) Dalton Trans 41:4249
16. Cortés CB, Galván VT, Pedro SS, García TV (2011) Catal Today 172:21
17. Trasarti AF, Marchi AJ, Apesteguía CR (2004) J Catal 224:484
18. Oertling H, Reckziegel A, Surburg H, Bertram H (2007) Chem Rev 107:2136
19. Nie Y, Jaenicke S, Chuah G (2009) Chem Eur J 15:1991
20. Yuasa Y, Tsuruta H, Yuasa Y (2000) Org Process Res Dev 4:1999
21. Vanek T, Novotny M, Podlipna R, David S, Valterova I (2003) J Nat Prod 66:1239
22. Cheng H, Meng X, Liu R, Hao Y, Yu Y, Cai S, Zhao F (2009) Green Chem 11:1227
23. Moreira JA, Corre AG (2003) Tetrahedron Asymmetry 14:3787
24. Porta R, Benaglia M, Puglisi A (2016) Org Process Res Dev 20:2
25. De Souza ROMA, Watts P (2017) J Flow Chem 7:146
26. Akwi F, Watts P (2018) Chem Commun 54:13894
27. Hughes DL (2018) Org Process Res Dev 22:13
28. Sagandira CR, Watts P (2019) Beilstein J Org Chem 15:2577